SIF2004 Structural Integrity and Fracture. http://eprint.uq.edu.au/archive/00000836

Mixed-Mode Fracture Of Adhesively Bonded Joints

Naghdali Choupani, Lin Ye and Yiu-Wing Mai
Centre for Advanced Materials Technology, School of Aerospace, Mechanical and Mechatronic Engineering
J07, The University of Sydney, Sydney, NSW 2006, Australia

ABSTRACT: The study focuses on using fracture mechanics to evaluate mixed-mode fracture properties of adhesively bonded aerospace material systems. As a part of experimental efforts, mixed-mode fracture tests were performed using modified Arcan specimens consisting of several combinations of adhesive, composite and metallic adherends using a special loading device. By varying the loading angle,α from 0^o to 90^o, mode I, mixed-mode and mode II fracture data were obtained experimentally. Experimental and theoretical studies of mixed-mode fracture behaviour of adhesively bonded aluminium, steel and CF/PEI composite joints were also performed using an adhesive in the aerospace industry. Finite element analyses were carried out on specimens with different adherends. Based on those analyses, mixed-mode fracture criterions for the adhesively bonded systems under consideration have been determined.

1 INTRODUCTION

Adhesively bonded joints and bonded repairs made to cracked metallic structures have been continuously receiving attention in the aerospace industry for the purpose of enhancing the fatigue resistance and restoring the stiffness and strength of damaged/cracked structures. Although stress-based approaches, which focuses on indicating both shear and normal (peel) stresses, have been the subject of a vast amount of research, fracture mechanics has also been proven to be a viable tool for adhesively bonded joint analysis. Fracture mechanics deals with the effects of flaws and fatigue in the presence of cracks [Kinloch, 1987]. A number of test methods have been proposed by many researchers to determine fracture toughness of adhesively bonded joints. The double cantilever beam (DCB) test is the most widely used method for measuring mode-I (opening) fracture toughness. The end-notched flexure (ENF) has emerged as one of the most convenient mode-II (shear) type cracking [Glyn et al, 1997]. Various attempts have been made to characterize fracture toughness under mixed-mode loading conditions in adhesively bonded joints, but mostly beam type specimens were used. The crack lap shear (CLS) and the mixed-mode bending (MMB) test specimens have been proposed by combining the schemes used for DCB and ENF tests to study the mixed mode fracture of bonded joints [Ducept et al, 1999]. However, for these test methods there are problems to create a wide range of mixed-mode ratios which limit their usefulness. Also, different beam type specimens would be required in order to obtain reliable results for fracture toughness in pure mode-I, pure mode-II, and mixed- mixed-mode loading conditions [Rikards, 2000].

Previous work at CAMT in this area has centered on the double cantilever beam (DCB) and double-lap and lap-strap joints [Yan et al, 2001]. However, deeper understanding of the fracture behavior of adhesively bonded joints, and particularly under mixed mode loading conditions, is needed in order to fully achieve the benefits of adhesive bonding [Pang, 1995]. In this work, a modified version of Arcan specimen is made for the mixed-mode fracture test of adhesively bonded joints, which allows mode-I, mode-II, and almost any combination of mode-I and mode-II loading to be tested with the same test specimen configuration [Arcan et al, 1978]. Therefore, the limitations presented in the previous mixed-mode toughness test methods can be avoided.

2 EXPERIMENTAL PROCEDURES

2.1 Material

This study examined a number of different substrates including aluminum, steel and CF/PEI composite. Although there are no such bonded structures on the aerospace applications, it was decided to investigate the mixed mode fracture of these bonded systems to better understand the behavior of the

FM® 300-2 adhesive and to calculate the effect of adherends. FM® 300-2 is a high strength rubber modified film adhesive widely used for bonding composite structures in aerospace bonding applications. The adhesive were processed according to the manufacturer's specification. A non-adhering film was inserted in the middle of the adhesive layer in order to introduce a starter crack. The composite adherend was a woven plate consisting of 12 plies of CF/PEI prepergs, in order to obtain a plate thickness of approximately 3mm. The prepergs were laid up by hand to the required number of plies and were produced using hot press. The specimens were cut with a diamond wheel and machined to the dimensions of 30x10x3 mm. The elastic constants of adherends and adhesive used in FEM analyses are summarized in Table 1. The CF/PEI composite is similar to the material investigated previously [Choupani et al, 2004], where 1 is the direction parallel to the fiber and 2 and 3 are the directions transverse to the fibers, while the direction of the crack coincides with the fiber direction (Figure 1).

Table I Elastic Properties of adhesive and adherends.

Material	E_1 [GPa]	E_2 [GPa]	E_3 [GPa]	G_{12} [GPa]	G_{13} [GPa]	G_{23} [GPa]	υ_{12}	υ_{13}	υ_{23}
FM® 300-2	2.3	2.3	2.3	0.8	0.8	0.8	0.4	0.4	0.4
Aluminum	72	72	72	27	27	27	0.3	0.3	0.3
Steel	207	207	207	79.6	79.6	79.6	0.3	0.3	0.3
CF/PEI	57.6	57.6	8.7	3.1	2.8	2.8	0.03	0.4	0.4

2.2 Test method and setup

The loading device and modified version of Arcan specimen are shown In Figure 1. The composite strip was attached into aluminum plates using adhesive. Bonding was carried out using a special jig to ensure alignment of the specimen halves. Steel substrates were polished prior to bonding using sand paper and degreased by an alkaline solution. For surface preparation of aluminum plates, FPL-Etch method was applied [ASTM, 1995]. Composite surface preparation method involved degreasing with methyl ethyl ketone (MEK), rinse and check for water break, hand abrasion with 320 grit aluminum oxide abrasive papers and clean for bonding [Daghyani et al, 1995]. The specimens were pinned into the loading device in order to transmit the applied loads. With the application of load P and by varying the loading angle,α from 0^o to 90^o , pure mode-I, pure mode-II, and all mixed- mode loading conditions can be created and tested. Fracture tests were conducted by controlling the constant displacement rate of 0.5 mm/min and the fracture loads and displacements were recorded. All tests were carried out using an Instron 5567 testing machine. Tests were repeated at least 3 times for each loading angle. The load-displacement curves generated by the test machine were used to determine maximum loads and displacement (Figure2). After testing, optical microscopy was used to examine the appearance of the fracture surface.

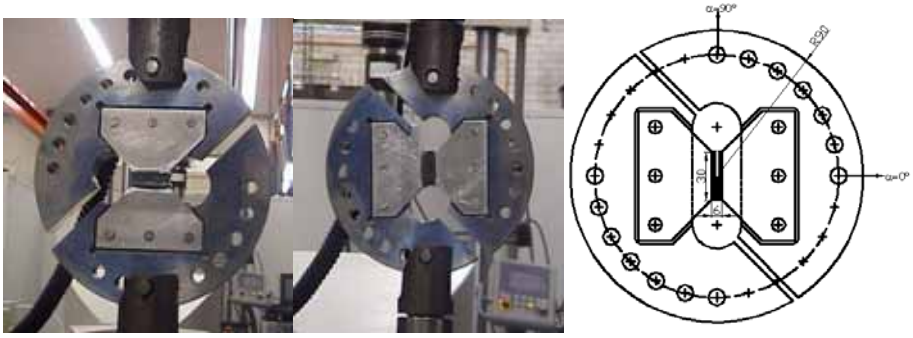

(a) **(b)** **(c)**

Figure 1 Overview of test rig and set up: (a) Mode-I test; (b) Mode-II test; (c) Geometry of the test fixture

3 ANALYSIS OF MIXED-MODE FRACTURE

The energy release rates for isotropic material can be calculated from the following relationships:

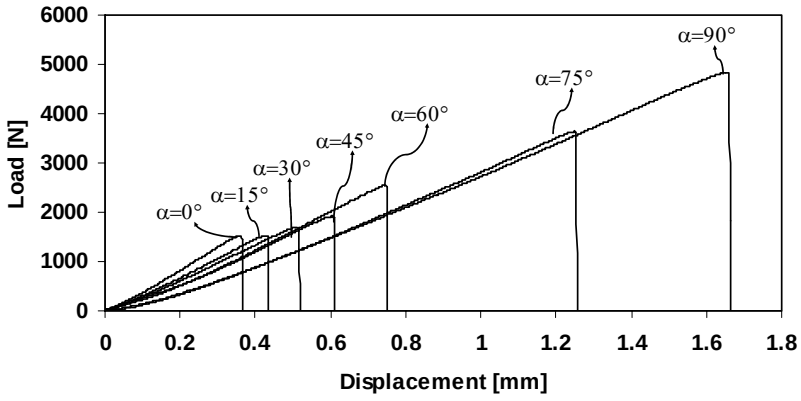

FIGURE 2 typical load-displacement relationships for adhesive with aluminum adherends

$$G_I = K_I{}^2 / \overline{E}, \qquad G_{II} = K_{II}{}^2 / \overline{E} \tag{1}$$

where $\overline{E} = E$ for plane stress, $\overline{E} = E/(1-\nu^2)$ for plane strain conditions, K_I and K_{II} are mode-I and mode-II stress intensity factors, respectively.

The stress intensity factors ahead of the crack tip for a modified version of Arcan specimen were calculated by using the following equations:

$$K_I = \frac{P_c\sqrt{\pi a}}{wt}\cos\alpha\, f_1(a/w), \qquad K_{II} = \frac{P_c\sqrt{\pi a}}{wt}\sin\alpha\, f_2(a/w) \tag{2}$$

where P_c is critical load at fracture, α is loading angle, w is specimen length, t is specimen thickness and a is crack length. In turn K_I and K_{II} are obtained using geometrical factors $f_1(a/w)$ and $f_2(a/w)$, respectively, which are obtained through finite element analysis of Arcan test specimen.

In the context of quasi-static analysis the J-integral in two dimensions is defined as:

$$J = \lim_{\Gamma\to 0}\int_\Gamma \mathbf{n}\cdot\left(W\mathbf{I} - \boldsymbol{\sigma}\cdot\frac{\partial\mathbf{u}}{\partial\mathbf{x}}\right)\cdot\mathbf{q}\,d\Gamma \tag{3}$$

where Γ is an arbitrary contour, W is the elastic strain energy for elastic material, q is a unit vector in the virtual crack extension direction, n is the outward normal to Γ, σ is the stress tensor and u is the displacement vector, as shown in Figure 3. The method used to calculate the stress intensity factor was an interaction integral method performed in ABAQUS, and is required to separate the components of the stress intensity factors in conjunction of finite element analysis. In the interaction integral method [Habbit et al, 2001; Sukumar, 2004], the two-dimensional auxiliary fields are introduced and superposed on the actual fields. By judicious choice of the auxiliary fields, the interaction integral can be directly related to the stress intensity factors $\mathbf{K} = 4\pi\mathbf{B}\cdot\mathbf{J}_{\text{int}}$ where $\mathbf{J}_{\text{int}} = [J^I_{\text{int}}, J^{II}_{\text{int}}, J^{III}_{\text{int}}]^T$. Based on the definition of the J-integral, the interaction integrals $\mathbf{J}^\alpha_{\text{int}}$ can be expressed as:

$$J^\alpha_{\text{int}} = \lim_{\Gamma\to 0}\int_\Gamma \mathbf{n}\cdot\left(\sigma : \varepsilon^\alpha_{aux}\mathbf{I} - \boldsymbol{\sigma}\cdot\left(\frac{\partial\mathbf{u}}{\partial\mathbf{x}}\right)^\alpha_{aux} - \sigma^\alpha_{aux}\cdot\frac{\partial\mathbf{u}}{\partial\mathbf{x}}\right)\cdot\mathbf{q}\,d\Gamma \tag{4}$$

The subscript *aux* represents three auxiliary pure Mode I, Mode II, and Mode III crack-tip fields for α=I, II, III, respectively. The domain form of the interaction integral is:

$$J^\alpha_{\text{int}} = -\int_A\left(\sigma_{ik}\varepsilon^{aux}_{ik}\delta_{1j} - \sigma_{ij}u^{aux}_{i,1} - \sigma^{aux}_{ij}u_{i,1}\right)q_{,j}\,dA \tag{5}$$

Figure 3 shows example of the mesh pattern of the specimen, which were performed with ABAQUS. The entire specimen with the initial crack a was modeled using eight node collapsed quadrilateral element and the mesh was refined around crack tip, so that the smallest element size found in the crack tip elements was approximately 0.05mm. A linear elastic finite element analysis was performed under

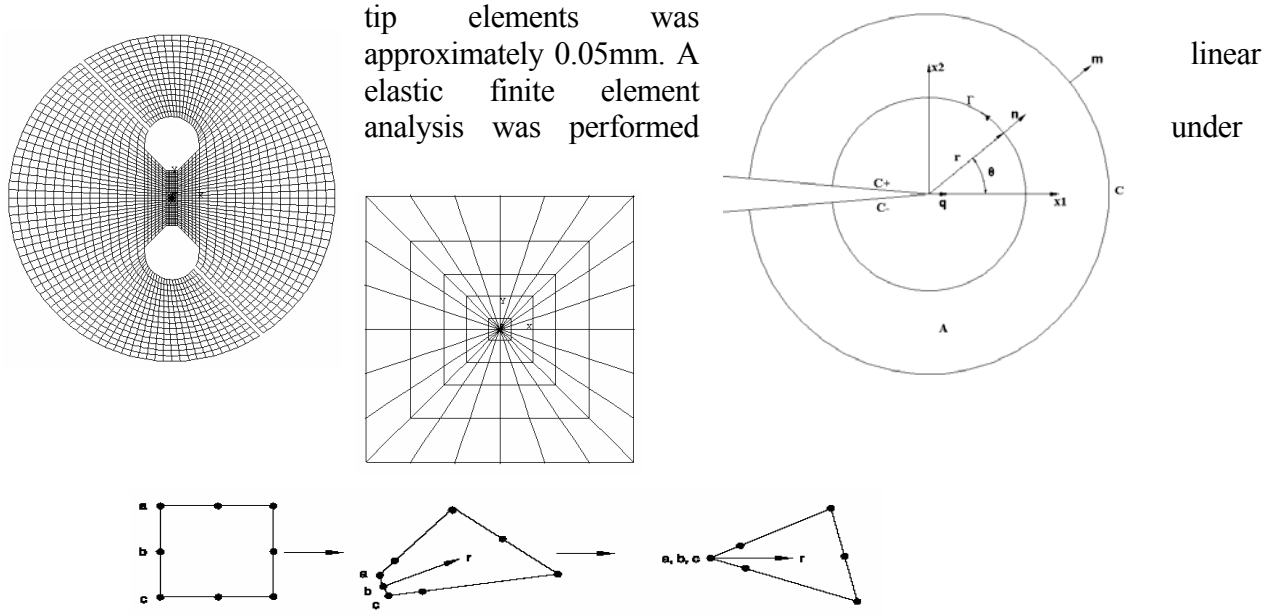

Figure 3 Finite element mesh pattern of the entire specimen and around the crack tip

a plane strain condition using $1/\sqrt{r}$ stress field singularity. To obtain a $1/\sqrt{r}$ singularity term of the crack tip stress field, the elements around the crack tip were focused on the crack tip and the mid side nodes were moved to a quarter point of each element side (as in Figure 3). If nodes a, b, and c are constrained to move together by specifying the same node number in the list of nodes forming the element, the strains and stresses are square root singular (suitable for linear elasticity).

4 RESULTS AND DISCUSSION

In order to assess stress intensity factors at fracture, K_I and K_{II} using Equations (2), geometrical factors $f_1(a/w)$ and $f_2(a/w)$ for both loading modes were determined. The a/w ratio was varied between 0.3 and 0.7 at 0.1 intervals and a fourth order polynomial was fitted through finite element analysis as (for aluminum substrate):

$$f_1(a/w) = -46.629\,(a/w)^4 + 122.6\,(a/w)^3 - 99.632\,(a/w)^2 + 33.767\,(a/w) - 3.7013$$
$$f_2(a/w) = 45.822(a/w)^4 - 90.463\,(a/w)^3 + 65.834\,(a/w)^2 - 20.617\,(a/w) + 2.6447 \quad (6)$$

It is of interest to compare the non-dimensional stress intensity factors for different substrates under different loading angles. In Figure 4, it can be seen for all adherends that for loading angles $\alpha \leq 60^o$, the mode-I fracture becomes dominant. As mode-II loading contribution increases, f_1 decreases and f_2 increases. For $\alpha \geq 75^o$ mode-II fracture becomes dominant. Adherends with different properties were found to have significant effects on the stress intensity factors that decrease as the adherend modulus increases. The difference between the modes-I stress intensity factors decreases as load application angle, α increases, while mode-II stress intensity factors exhibits the opposite trend.

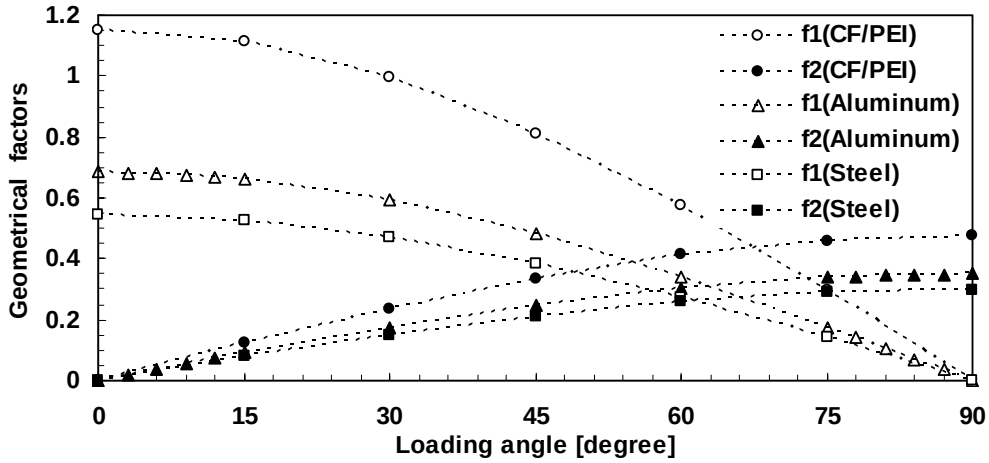

Figure 4 Geometrical factors vs. loading angle,α for different adherends

The energy release rates were calculated using conventional Equations (1) and the calculated mixed-mode ratios of energy release rates for aluminum substrates are shown in Table 2. The relationship between the mixed-mode ratios of energy release rates and the loading angles α is presented in Figure 5. For loading angles close to pure mode-I loading, very high ratios of mode-I to mode-II is dominant. The ratios of strain energy release rates close to pure mode-II loading exhibits the opposite trend. It confirms that by varying the loading angle of Arcan specimen pure mode-I, pure mode-II and a wide range of mixed-mode loading conditions can be created and tested.

Table II Mixed-mode ratios of energy release rates for aluminum adherends

α	0°	3°	6°	9°	12°	15°	30°	45°	60°	75°	78°	81°	84°	87°	90°
G_{II}/G_I	0	0.0007	0.003	0.007	0.01	0.02	0.09	0.3	0.8	3.7	5.9	10.6	24.4	101.1	∞

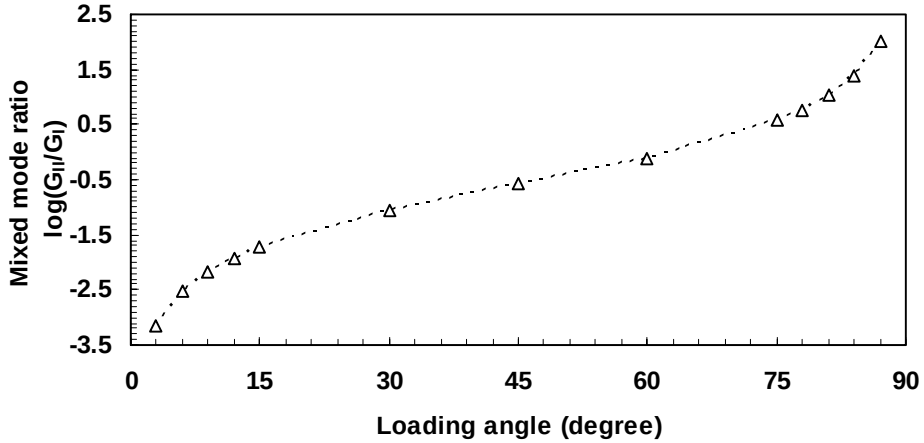

Figure 5 The ratio of mode-II to mode-I, G_{II}/G_I (in logarithmic scale), vs. loading angle,α for aluminum adherends

Figure 6 shows G_{IC}, G_{IIC} and G_{TC} =G_{IC}+G_{IIC}, obtained by experiments for different adherends under various loading conditions. Mode-I and Mode-II fracture toughness of aluminum substrate specimens were approximately 210 J/m^2 and 550 J/m^2, respectively. The fracture path was generally cohesive in this system for all loading conditions, suggesting that surface preparation of the adherends were adequate. Joints with steel and composite adherends showed lower fracture toughness under all modes of loading. Mode-I and Mode-II fracture toughness of the steel and composite systems were 80 J/m^2, 279 J/m^2 and 153 J/m^2, 235 J/m^2, respectively. Crack growth in the steel specimens was almost cohesive, but the crack meandered from one interface to the other with no distinct pattern. In composite

adherends, the crack often departed from the adhesive layer and appeared to occur in the matrix layer of the composite strap within the plies nearest the bond line and a small number of fibers embedded in the adhesive remaining on the adherend (Figure 7).

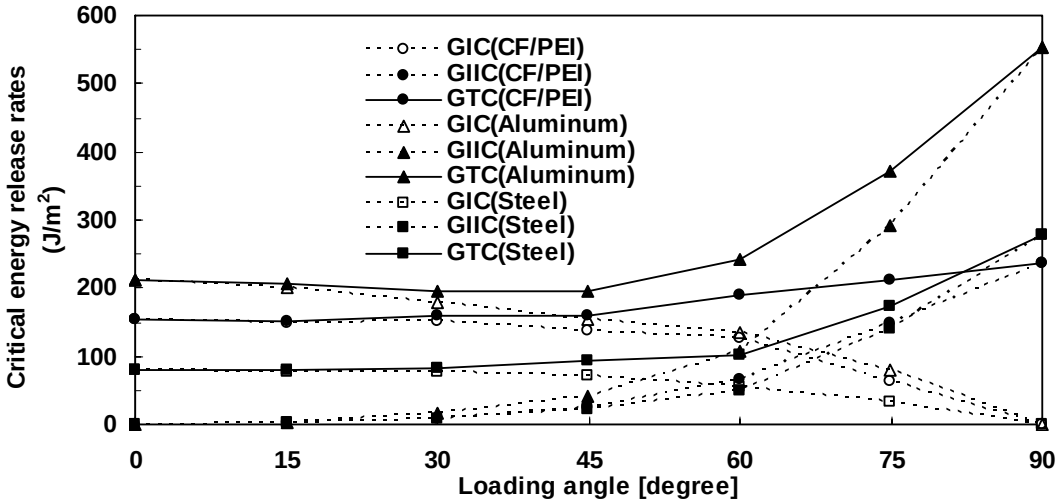

Figure 6 Experimental results of G_{IC}, G_{IIC}, $G_{TC}=G_{IC}+G_{IIC}$ vs. loading angle,α for different adherends

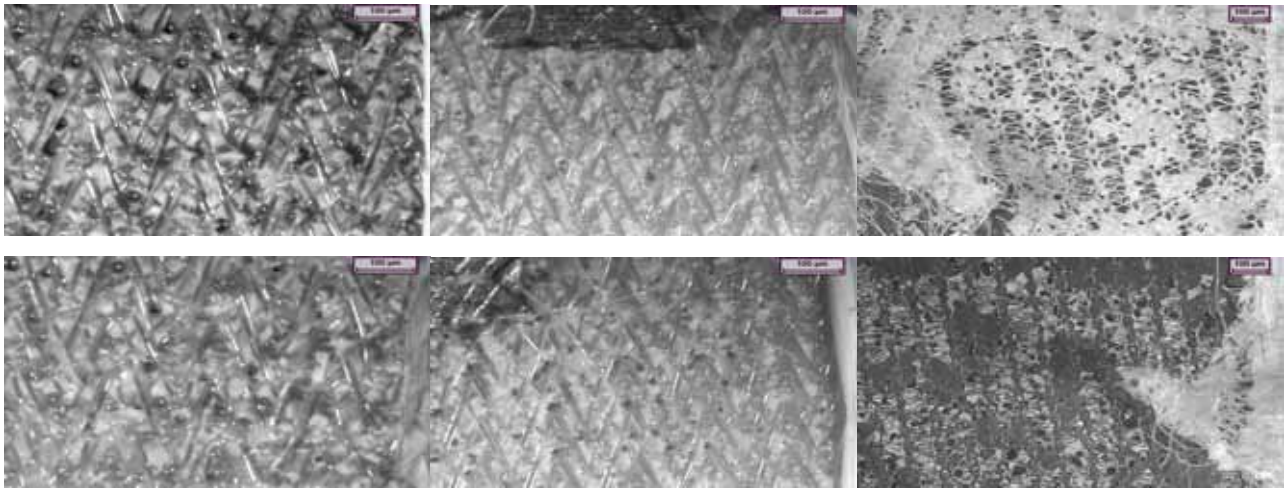

(a) **(b)** **(c)**

Figure 7 Fracture surfaces: (a) Aluminum adherends; (b) Steel adherends; (c) CF/PEI adherends

5 CONCLUSION

In this paper the mixed-mode fracture behavior for adhesively bonded joints constructed of several combinations of adhesive, composite and metallic adherends was investigated based on experimental and numerical analyses. A modified version of Arcan specimen was employed to conduct mixed-mode test using the special test loading device. The full range of mixed-mode loading conditions including pure mode-I and pure mode-II loading can be created and tested. It is a simple test procedure, clamping/unclamping the specimens is easy to achieve and only one type of specimen is required to generate all loading conditions. Results of joints with steel and composite adherends showed lower fracture toughness under all modes of loading.

REFERENCES

Arcan, M., Z. Hashin, and A. Voloshin. "A Method to Produce Plane-stress States with Applications to Fiber-reinforced Materials," *Experimental Mechanics,* 18:141-6, 1978.

ASTM Standard D2651-90, "Standard Guide for Preparation of Metal Surfaces for Adhesive Bonding", 1995

Choupani, N., L. Ye, and Y.-W. Mai. "Mixed Mode Fracture of a CF/PEI Composite Material," in *Proceedings of the 4th Asian-Australasian Conference on Composite Materials*, 6-9 July 2004, Australia, pp 403-409, 2004.

Daghyani, H. R., L. Ye, and Y.-W. Mai. "Mixed-mode Fracture of Adhesively Bonded CF/Epoxy Composite Joints," *J. Compos. Mater*, 30:1248-65, 1996.

Ducept, F., D. Gamby, and P. Davies. "A Mixed-mode Failure Criterion Derived from Tests on Symmetric and Asymmetric Specimens," *Compos. Sci. Tech*., 59:609-619, 1999.

Glyn, L., L. Ye, Y.-W. Mai, and C.-T Sun. "The Effect of Adhesive Bonding between Aluminum and Composite Preperg on the Mechanical Properties of Carbon-fiber-reinforced Metal Laminates," *Compos. Sci. Tech*., 57:35-45, 1997.

Habbit, Karlsson and Sorensen. *ABAQUS User's Manual version 6.2.4*, 2001.

Kinloch, A. J. *Adhesion and Adhesives*: Science and Technology, Chapman and Hall, 1987.

Pang, H. L. J. "Mixed Mode Fracture Analysis and Toughness of Adhesive Joints. *Eng. Frac. Mech*., 51(4):575-83, 1995.

Rikards, R "Interlaminar Fracture Behaviour of Laminated Composites,"*Comp. and Structures,* 76:11-18, 2000.

Sukumar, Z. Y. Huang, J.-H. Prevost and Z. Suo, 'Partition of Unity Enrichment for Bimaterial Interface cracks', *Int. J. Numer. Meth. Engng*, 59:1075–1102, 2004.

Yan, C., Y.-W. Mai, Q. Yuan, L. Ye, J. Sun. "Effects of Substrate Materials on Fracture Toughness Measurement in Adhesive Joints", *Int. J. Mech. Sci.,* 43:2091-2102, 2001.